ISSN 0036-0295, Russian Metallurgy (Metally), Vol. 2016, No. 6, pp. 522–529. © Pleiades Publishing, Ltd., 2016.
Original Russian Text © G.G. Mikhailov, L.A. Makrovets, L.A. Smirnov, L.E. Dresvyankina, 2016, published in Elektrometallurgiya, 2016, No. 3, pp. 32–40.

THEORY OF METALLURGICAL PROCESSES

Analysis of the Fe–Ce–O–C–*M* Phase Diagrams (*M* = Ca, Mg, Al, Si) by Constructing a Component-Solubility Surface

G. G. Mikhailov[a], L. A. Makrovets[a, *], L. A. Smirnov[b], and L. E. Dresvyankina[c]

[a] *South-Ural State University, pr. Lenina 76, Chelyabinsk, 454080 Russia*
[b] *OAO Ural Institute of Metals, ul. Gagarina 14, Yekaterinburg, 620219 Russia*
[c] *ML NITs PAO Seversk Pipe Plant, ul. Botanicheskaya 19, Yekaterinburg, 620137 Russia*
**e-mail: tchla@mail.ru*

Received November 18, 2015

Abstract—Analysis of the ternary phase diagrams of Ce_2O_3- and CeO_2-containing oxide systems allowed us to find the oxide compounds that form during steel deoxidizing with cerium and with cerium together with aluminum, calcium, magnesium, or silicon. The temperature dependences of the equilibrium constants of formation of Ce_2O_3 oxides and $Ce_2O_3 \cdot Al_2O_3$, $Ce_2O_3 \cdot 11Al_2O_3$, $Ce_2O_3 \cdot 2SiO_2$, $7Ce_2O_3 \cdot 9SiO_2$ and $Ce_2O_3 \cdot SiO_2$ compounds are found. Surfaces for the component solubility in metallic melts Fe–Al–Ce–O–C, Fe-Ca–Ce–O–C, Fe–Mg–Ce–O–C, and Fe–Si–Ce–O–C are constructed. Nonmetallic inclusions that form in the course of experimental melts of St20 steel after its deoxidizing with silicocalcium and rare-earth metal (REM)-containing master alloys in a ladle furnace after degassing are studied. Phase inhomogeneity of the inclusions is found. As a rule, they consist of phases classified into the following three groups: oxide–sulfide, sulfide–oxide, and multiphase oxide–sulfide melt. Calcium aluminates are found to be components of complex sulfide-oxide noncorrosive inclusions.

DOI: 10.1134/S0036029516060100

Out-of-furnace treatment of steel is the most efficient technique for its refining and modification. After preliminary deoxidizing and desulfurization, the content of oxygen in steel is 10^{-4}–10^{-3} wt % and the residual sulfur content is slightly higher [1]. In this case, in addition to the formed specific slag medium, aluminum and alloys with calcium, aluminum, and silicon are used. At the final stages of refining, it is possible to apply alloys or mixtures of deoxidizers and modifiers, such as Si–Ca–Ba, Si–Ca–REM or multicomponent alloys, such as mishmetal and Inseel (NPP Tekhnologiya, Russia) [2]. When estimating the efficiency of action of complex alloys and mixtures with highly active elements, such as Ca, Ba, Mg, Ce, and La, in the presence of alloying components of steel (Mn, Cr, V, Ti, Ni, Mo), it is necessary to find the deoxidizing and modifying role of each of the highly active elements taking into account the results of preliminarily refining. In the present study, we consider the complex interaction between cerium and oxygen in a multicomponent metallic melt, namely, steel. A preliminary analysis of the composition of possible oxide phases formed as intermetallic inclusions [3–10] allowed us to conclude that the melt is in equilibrium with the oxide phases determined by the chemical reactions given in Table 1. The components of oxide melts are given in parenthesis, and compounds or oxides (components of oxide solid solutions) are given in square brackets. Preliminarily, binary and ternary oxide systems containing Ce_2O_3 and CeO_2 were carefully analyzed; liquidus and liquidus surfaces were constructed, which allowed us to determine the physical state of oxide phases interfaced with the metal. The thermodynamic properties of the components of oxide melts were determined according to the theory of subregular solutions with a common anion [11]. For associated systems, the energy parameters Q_{ijkl} were the following:

$FeO–Ce_2O_3–Al_2O_3$
(–90000, –90000, –90000 cal/mol);

$FeO–Ce_2O_3–Si_2O_3$
(–18000, –45000, –4000 cal/mol);

$FeO–SiO_2–CeO_2$
(–4000, +8000, +1000 cal/mol);

$Ce_2O_3–SiO_2–CeO_2$
(–45000, –12000, –15000 cal/mol);

$FeO–Ce_2O_3–CaO$
(–13794, –13794, –6897 cal/mol).

Table 1 shows available equations for equilibrium constants (temperature dependences) for corresponding reactions and analogous dependences for the reactions of formation of cerium aluminates and silicates, which were calculated by us. It should be noted that, at the temperatures of steel-making processes, the cerium valence is +3 and +4. When constructing a thermodynamic model of the interaction of cerium with oxygen, the compositions of equilibrium oxide phases were determined for the oxide systems adjacent to metal regions. In our opinion, in the case of the Fe–Ce–O phase triangle, we should consider the equilibrium corresponding to the conodes connecting the $FeO–Ce_2O_3$ quasi-binary system and the multiphase $Ce_2O_3–CeO_3$ equilibrium and, thus, take into account the possibility of valences of +3 and +4 for cerium participating in the formation of nonmetallic inclusions in both melt and solid. When modeling complex phase equilibria, we constructed the surfaces of melt component solubilities and showed the concentration boundaries of metal that are in equilibrium with the corresponding oxide phases. In this case, we solved transcendental equation systems, which characterize the component solubility for any equilibrium. The concentration limits of the metal compositions in equilibrium with one of the oxide phases having unchanged or variable composition are shown in the solubility surface areas. The metal compositions that are equilibrium with two oxide phases are shown by contrast lines. The points of intersection of the lines correspond to the equilibria between a metal and three oxide phases. This method is good because, in adding components, the surface of melt component solubility can be found using isocomposition sections of formed solubility hypersurfaces. These surfaces of component solubility in a liquid metal sufficiently clearly retain a diagram profile and, at the same time, give the possibility for appearance of more complex phase equilibria in them at the expense of the fact that, in our opinion, the constructed diagrams of the oxide systems $FeO–Ce_2O_3–CeO_2$, $FeO–Ce_2O_3–Al_2O_3$, $FeO–Ce_2O_3–SiO_2$, $FeO–SiO_2–CeO_2$, $Ce_2O_3–SiO_2–CeO_2$, $FeO–Ce_2O_3–CaO$, $FeO–CeO_2–CaO$, $FeO–Ce_2O_3–MgO$, and $FeO–CeO_2–MgO$ are known. Using these diagrams, the corresponding Fe–Ce–Ca–O, Fe–Ce–Mg–O, Fe–Ce–Al–O, and Fe–Ce–Si–O phase diagrams were calculated and constructed, and the effect of carbon on the aforementioned phase equilibria was shown as well.

Figure 1 shows the surfaces of component solubility in liquid iron for the Fe–Ce–Ca–O and Fe–Ce–Ca–O–C systems at 1600°C at a pressure of 1 atm. The compositions of liquid metal in equilibrium with the crystalline CeO_2 oxide and Ce_2O_3 are given in areas I and II, respectively. The compositions of liquid metal in equilibrium with CaO containing a small amount of FeO and with oxide melt (FeO, CaO, Ce_2O_3, CeO_2) are given in areas III and IV, respectively. Under line *nps* (see Fig. 1a), the compositions of liquid metal in equilibrium with the Ca vapor are given; the *nps* line gives the compositions of metal in equilibrium with either the Ca vapor and the solid CaO oxide (*np*) or the solid Ce_2O_3 oxide (*ps*). In area VI, the liquid metal is in equilibrium with the oxide melt (FeO, CaO, Ce_2O_3, CeO_2). Figure 1b shows the surface of melt component solubility for the Fe–Ce–Ca–O–C system. Here, two composition areas of metal, which is in equilibrium with vapor consisting mainly of Ca vapor with CO and CO_2 impurities (area VII) and of CO and CO_2 with small Ca vapor impurity (area VIII), should be noted.

Figure 2 shows the surface of melt component solubility for the Fe–Ce–Mg–O and Fe–Ce–Mg–O–C systems. The structure of the surfaces slightly differs

Table 1. Temperature dependences of the equilibrium constants of reactions [12, 13]

Reaction	$\log K = -A/T + B$	
	A	*B*
$(FeO) = [Fe] + [O]$	6320	4.734
$(Ce_2O_3) = 2[Ce] + 3[O]$	64128	17.816
$(CeO_2) = [Ce] + 2[O]$	39540	11.99
$(Al_2O_3) = 2[Al] + 3[O]$	58320	18.02
$(SiO_2) = [Si] + 2[O]$	30225	11.56
$(MgO) = [Mg] + [O]$	22457	6.54
$(CaO) = [Ca] + [O]$	31480	12.55
$\lvert Ce_2O_3\rvert = 2[Ce] + 3[O]$	68500	19.60
$\lvert CeO_2\rvert = [Ce] + 2[O]$	43694	13.55
$\lvert SiO_2\rvert = [Si] + 2[O]$	31100	12.00
$\lvert Al_2O_3\rvert = 2[Al] + 3[O]$	64000	20.48
$\lvert FeO\rvert = [Fe] + [O]$	8069	5.80
$\lvert MgO\rvert = [Mg] + [O]$	26500	7.85
$\lvert CaO\rvert = [Ca] + [O]$	34103	13.46
$\lvert FeO \cdot Al_2O_3\rvert = [Fe] + 2[Al] + 4[O]$	74580	26.37
$\lvert Ce_2O_3 \cdot Al_2O_3\rvert = 2[Ce] + 2[Al] + 6[O]$	149214	43.736
$\lvert Ce_2O_3 \cdot 11Al_2O_3\rvert = 2[Ce] + 22[Al] + 36[O]$	801014	252.396
$\lvert Ce_2O_3 \cdot SiO_2\rvert = 2[Ce] + [Si] + 5[O]$	104758	32.055
$\lvert 7Ce_2O_3 \cdot 9SiO_2\rvert = 14[Ce] + 9[Si] + 39[O]$	765945	233.031
$\lvert Ce_2O_3 \cdot 2SiO_2\rvert = 2[Ce] + 2[Si] + 7[O]$	130689	41.180
$\{CO\} = [C] + [O]$	1168	−2.07
$\{CO_2\} = [C] + 2[O]$	9616	2.51
$\{Ca\} = [Ca]$	−1912	−2.69
$\{Mg\} = [Mg]$	−6670	−6.48

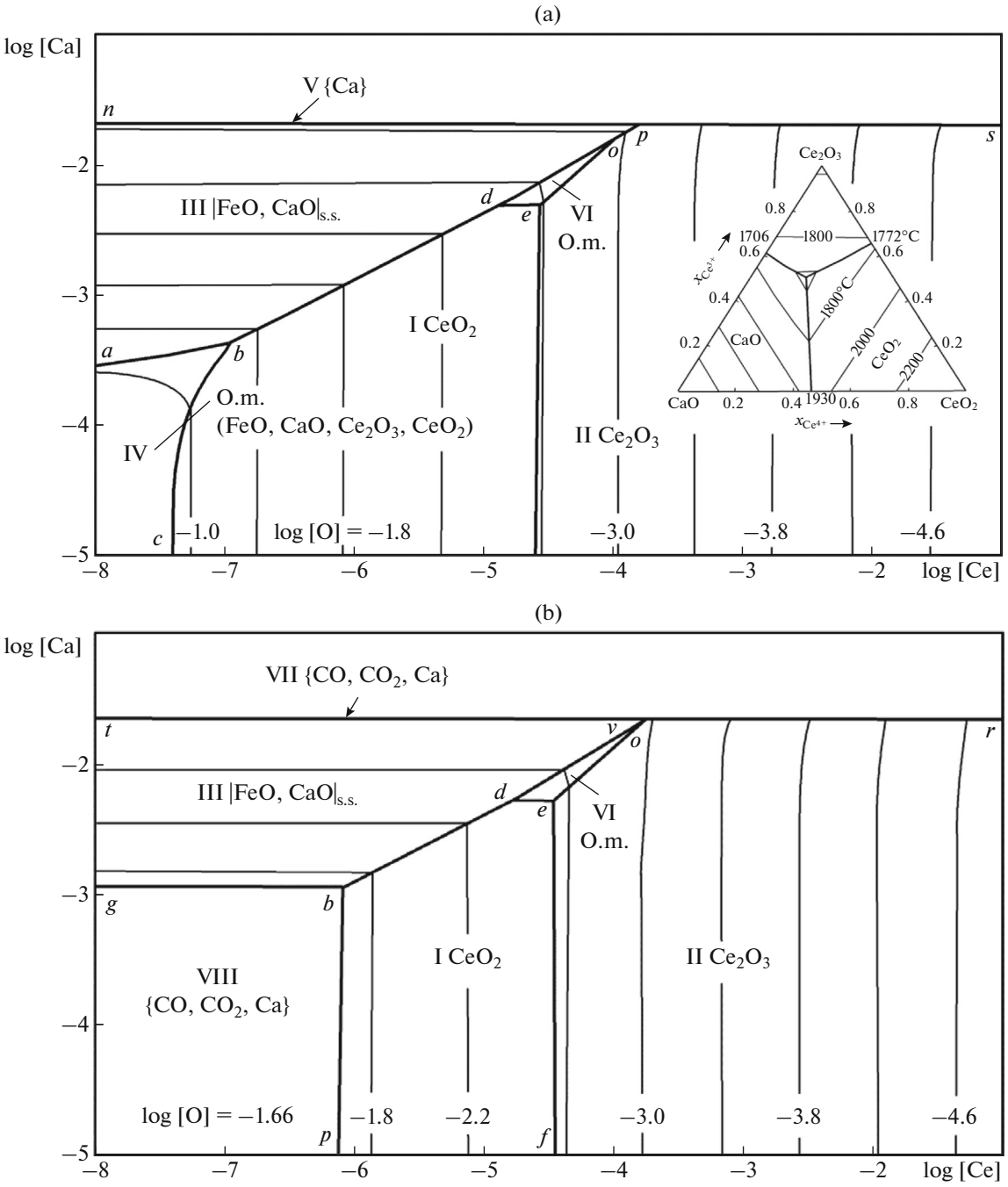

Fig. 1. Surface of melt component solubility for the Fe–Ca–Ce–O–C system at $T = 1600$°C and $P_{tot} = 1$ atm: (a) [C] = 0 and (b) [C] = 0.1 wt %.

from the Fe–Ce–Ca–O and Fe–Ce–Ca–O–C phase diagrams. In our opinion, some differences in the coordinates of solubility areas are related to the higher deoxidizing capcity of magnesium and its higher vapor pressure.

Figure 3 shows the surface of melt component solubility for the Fe–Al–Ce–O–C system. It follows from the Al_2O_3–Ce_2O_3 and FeO–Ce_2O_3–Al_2O_3 phase diagrams that the solubility surface for the Fe–Al–Ce–O–C system should contain composition areas of metal that is in equilibrium with the compounds $Ce_2O_3 \cdot Al_2O_3$ (area IV) and $Ce_2O_3 \cdot 11Al_2O_3$ (area V). It is seen from Fig. 3 that the deoxidizing capacity of cerium is higher than that of aluminum. Cerium blocks the formation of corundum at a very low aluminum concentration in the metal. In this case, the

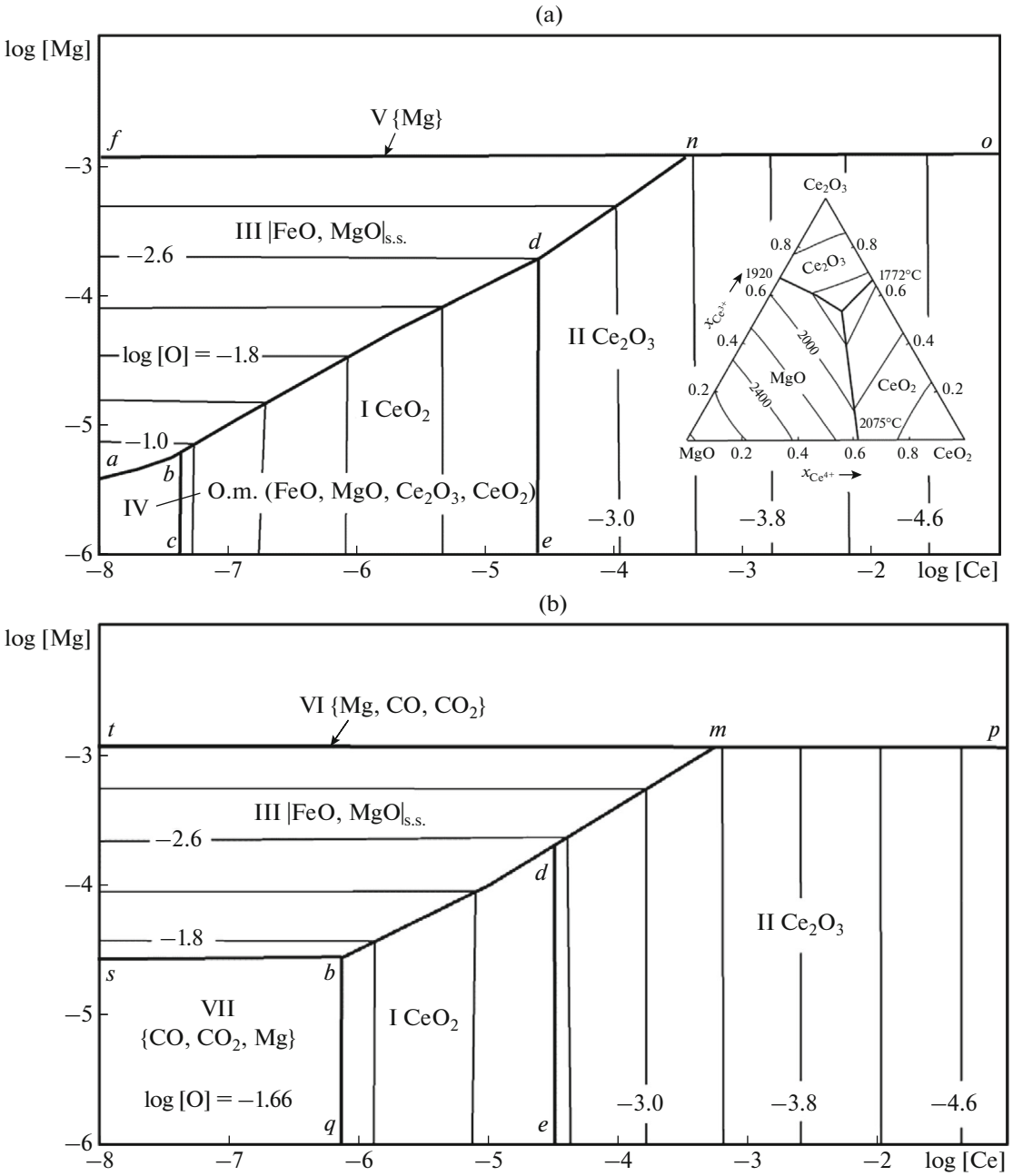

Fig. 2. Surface of melt component solubility for the Fe–Mg–Ce–O–C system at $T = 1600$°C and $P_{tot} = 1$ atm: (a) [C] = 0 and (b) [C] = 0.1 wt %.

cerium concentration is 10^{-6}–10^{-8} wt %. At a common aluminum concentration in the metal of 10^{-3} wt % and a cerium concentration in the metal of 10^{-6}–10^{-3} wt %, the complex $Ce_2O_3 \cdot Al_2O_3$ and $Ce_2O_3 \cdot 11Al_2O_3$ compounds are formed as nonmetallic inclusions.

Figure 4 shows the Fe–Ce–Si–O and Fe–Ce–Si–O–C diagrams. It follows from the appearance of surface of melt component solubility and the constructed $FeO–Ce_2O_3–SiO_2$, $FeO–SiO_2–CeO_2$, and $Ce_2O_3–SiO_2–CeO_2$ oxide diagrams that oxide melts (area I), silica (area II), $Ce_2O_3 \cdot 2\ SiO_2$ (area III) and $Ce_2O_3 \cdot SiO_2$ (area IV) cerium silicates, and CeO_2 (area V) and Ce_2O_3 (area VI) solid oxides can form as equilibrium oxide phases. In the case of the presence of carbon, the liquid metal can also be in equilibrium with vapor {CO, CO_2} (Fig. 4b). The possibility of formation of

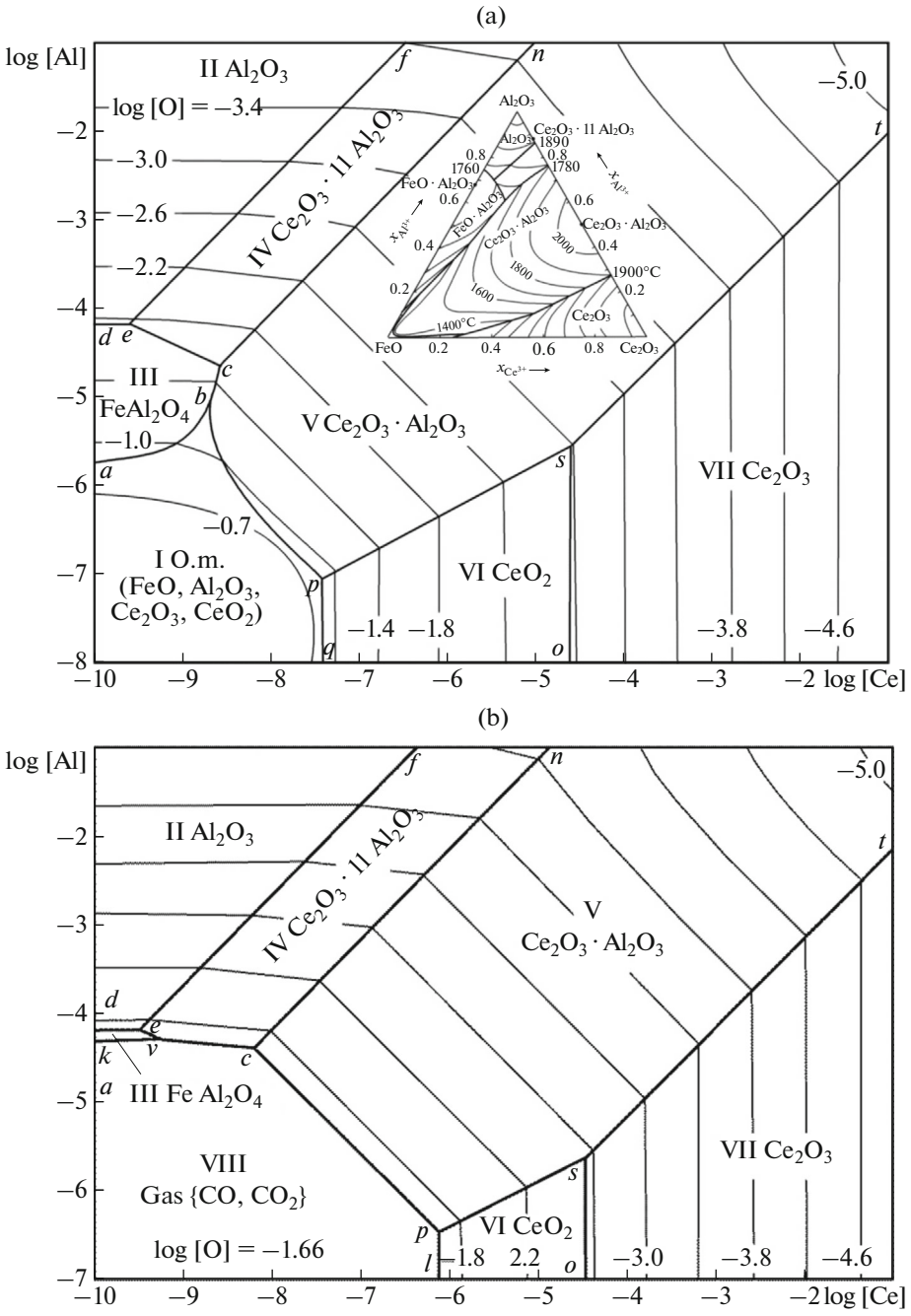

Fig. 3. Surface of melt component solubility for the Fe–Al–Ce–O–C system at $T = 1600$°C and $P_{tot} = 1$ atm: (a) [C] = 0 and (b) [C] = 0.1 wt %.

silica–cerium oxide complexes is realized at silicon concentrations in the metal of at least several ten thousandth fractions of a percent.

The appearance of the considered diagrams indicates that nonmetallic inclusions, which are formed at the final stages of refining of liquid steel in adding silicocalcium and REM alloys after steel degassing, should be multiphase and fine, since the deoxidizers are added to the metal containing oxygen (several ten thousandth fractions of a percent) and sulfur (several thousandth fractions of a percent). Experiments related to the optimization of deoxidation and modification processes with powder wires filled with silicocalcium and complex Forsteel 12c and FS30REM3OA modifiers were performed at the Seversk pipe plant. After degassing and continuous casting, templates were studied with

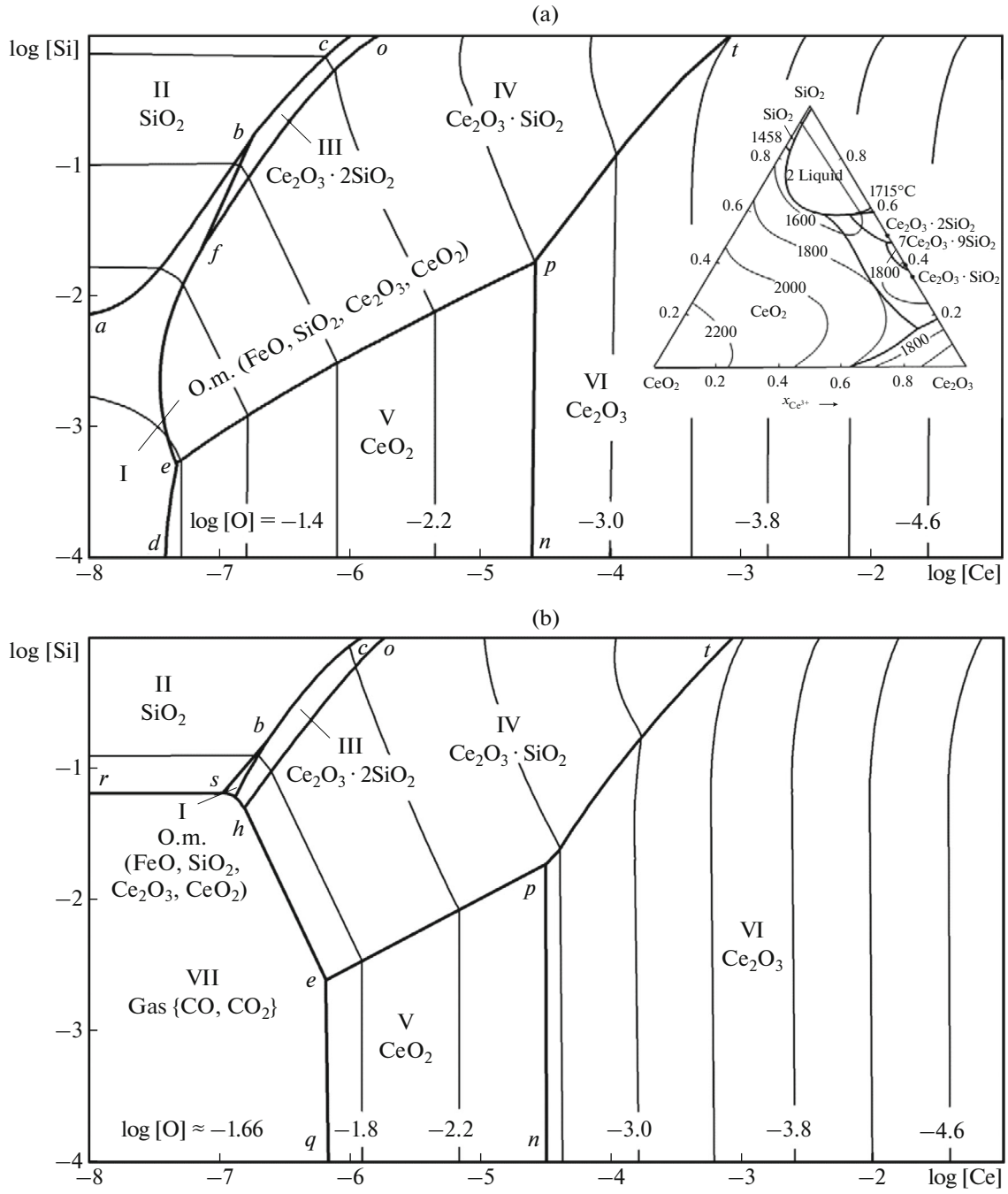

Fig. 4. Surface of melt component solubility for the Fe–Si–Ce–O–C system at $T = 1600$°C and $P_{tot} = 1$ atm: (a) [C] = 0 and (b) [C] = 0.1 wt %.

a JEOL JSM-6460LV electron microscope. Metallic inclusions were multiphase and mainly 1–5 μm in size. Figure 5 shows the appearance of such an inclusion. Table 2 gives the chemical analysis data obtained by scanning electron microscopy (SEM). A multiphase inclusion was also subjected to electron-beam scanning. Thus, it was found that, according to the chemical composition, the inclusion comprises several phase components. An oxide-based phase is clearly observed; it was detected from aluminum, oxygen, and magnesium spectra. A portion of inclusion (zone corresponding to point *2*) is likely to be magnesium spinel–based oxide phase in the form of solution, in which calcium, cerium, and lanthanum aluminates are present. Based on sulfur, calcium, and manganese spectra, we conclude that the area corresponding to

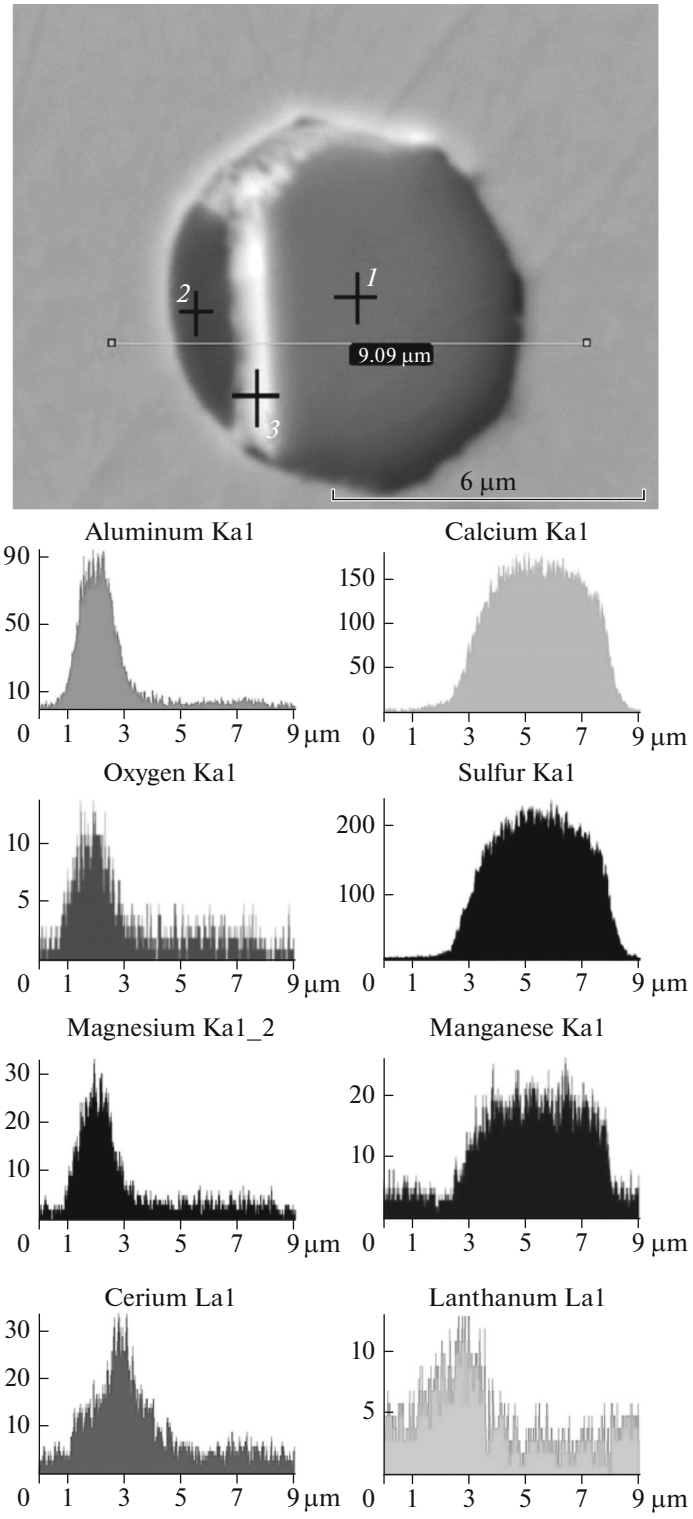

Fig. 5. Appearance of a typical nonmetallic inclusion in the steel refined with REM and SEM spectra of elements.

point *3* consists of calcium, manganese, and cerium sulfides. The area around point *3* corresponds to the formation of calcium, manganese, and cerium sulfides. The area around point *3* corresponds to the interaction of almost all impurity components with oxygen and sulfur. It is likely that this is related to the appearance of liquid fluid oxide-sulfide phase during the formation of inclusions. The compounds that are

Table 2. Chemical analysis data for the inclusion in Fig. 5

Point	Element, at %												
	O	Mg	Al	Si	S	Ca	Mn	Fe	Y	La	Ce	Nd	Total
1	–	–	–	–	46.55	43.56	6.56	2.19	–	–	1.14	–	100.0
2	47.99	10.65	28.13	–	0.92	1.51	–	8.36	–	–	2.43	–	100.0
3	38.13	5.98	17.76	–	14.90	9.78	1.59	2.37	0.62	1.71	6.62	0.55	100.0

present after solidification are cerium, magnesium, and calcium oxides; silicates; and aluminates. This statement is confirmed by our thermodynamic calculations. The sulfide component was determined by electron microprobe analysis of steel components.

CONCLUSIONS

(1) The surfaces of melt component solubility for the Fe–Al–Ce–O–C, and Fe–Ca–Ce–O–C, Fe–Mg–Ce–O–C, and Fe–Si–Ce–O–C systems were constructed.

(2) It was found that, when adding complex deoxidizers and modifiers containing cerium, the formation of cerium aluminides and silicates is possible. The formed calcium aluminides are dissolved in inclusions and are present in the form of fine phase elements.

(3) The use of cerium-group lanthanides added in the form of a powder wire and subsequent soft argon blowing before placing a ladle on the stand of continuous billet casting machine is the most promising technology. In this case, the castability of pipe steels (St20) increases and the formation of corrosive inclusions is excluded.

ACKNOWLEDGMENTS

This study was supported by the Russian Foundation for Basic Research (project no. 13-08-12167).

REFERENCES

1. Ya. E. Gol'dshtein and V. G. Mizin, *Refining of Iron and Steel* (Metallurgiya, Moscow, 1986).
2. I. V. Ryabchikov, *Modifiers and Technologies for Out-of-Furnace Treatment of Iron-Carbon Alloys* (Ekomet, Moscow, 2008).
3. G. G. Mikhailov and L. A. Makrovets, "Phase equilibria in liquid steel by adding cerium," Vestn. Uzhn. Ural Univer., Ser. Metall. **13** (2), 16–19 (2013).
4. A. I. Leonov, *High-Temperature Chemistry of Cerium–Oxygen Compounds* (Nauka, Leningrad, 1969).
5. D. A. Movenko, G. I. Kotel'nikov, A. E. Semin, et. al., Improvement of cerium treatment conditions of pipe steel," Electromet., No. 8, 7–12 (2012).
6. N. A. Toropov, V. P. Barzakovskii, V. V. Lapin, and N. N. Kurtseva, *Phase Diagrams of Silicate Systems. Handbook. Issue 1. Binary Systems* (Nauka, Leningrad, 1969).
7. L. M. Lopato, L. I. Lugin, and A. V. Shevchenko, "Phase relations in magnesium oxide-cerium-group REE oxide systems," Zh. Neorg. Khim., **16** (1), 254–257 (1971).
8. A. C. Tas and M. Akinc, "Phase relations in the Ce_2O_3–Al_2O_3 in inert and reducing atmospheres," J. Am. Ceram. Soc., **77** (11), 2953–2960 (1994).
9. A. C. Tas and M. Akinc, "Phase relations in the Ce_2O_3–Al_2O_3 in inert and reducing atmospheres," J. Am. Ceram. Soc., **77** (11), 2961–2967 (1994).
10. Yu. S. Sarkisov and I. A. Kurzina, *Phase Diagrams of Two-Component Systems. Workbook* (Izd. Tomskogo Arkhitekturnogo Univer., Tomsk, 2001).
11. G. G. Mikhailov and V. I. Antonenko, *Thermodynamics of Metallurgical Slags: Tutorial* (ID MISiS, Moscow, 2013).
12. I. S. Kulikov, *Deoxidation of Metals* (Metallurgiya, Moscow, 1975).
13. E. T. Turkdogan, *Physical Chemistry of High-Temperature Technology* (Academic Press INC, NY, 1980; Metallurgiya, Moscow, 1985).

Translated by N. Kolchugina